CFD MODELLING: OPTIMISATION OF THE NITROCELLULOSE NITRATOR

J. LEA[1,2], A.J. GEHRIG[1], P.S. FLAVEL[1] AND A.A. ADESINA[2,*]
[1] ADI – Military Propellants & High Explosives, Land Ordnance Unit
Level 18, 607 Bourke Street, Melbourne VIC 3000 Australia.

[2] Reactor Engineering and Technology Group, School of Chemical Engineering & Industrial Chemistry
The University of New South Wales, Sydney, NSW 2052 Australia.

* Corresponding author: a.adesina@unsw.edu.au

ABSTRACT

The manufacture of nitrocellulose, which is the basis of most artillery, rocket and missile propellant, is intrinsically risky due to the energetic nature of the product and the sensitivity of the process. To optimise the performance of the nitration unit, computational fluid dynamics (CFD) was employed to characterise the nitration unit and to provide detailed, relevant process data emanating from a new perspective. The actual nitration unit was scaled-down in order to use independent measurements from particle image velocimetry (PIV) to validate the CFD results. It was only after the model and simulation results were successfully validated that the characterisation of the actual unit was carried out. With the nitration unit characterised, its optimisation was carried out by performing modelling on different geometrical configurations with a view to selecting one which gives an optimum performance.

INTRODUCTION

There is always the inherent risk in the manufacture of military propellants such as nitrocellulose (NC) and high explosives, via the continuous nitration process. Because of such risks, it is not always that convenient to optimise the nitration unit by building a pilot-scale version or to conduct physical experiments in the actual plant. Inept experiments causing small incidents in such a conservative industry often lead to losses of a catastrophic magnitude. Apart from the safety aspect, an equally important motivation is the economic aspect where stopping production to conduct experiments, may be economically prohibitive. Despite such obstacles, to prevent the obsolescence of our technology due to the lack of optimisation or the failure of keeping up with advances in technology, there is little choice but to harness current and future technologies and apply them to our requirements. The primary objective of this study is to characterise the nitration unit so that relevant information is available to optimise the performance of this unit. Besides using the results from this study to optimise the unit, having the unit characterised means this unit can be understood thoroughly so that in the event a new plant is desired, the transfer of operation knowledge from the existing plant to the proposed plant will have less setbacks [1]. Most of the work was carried out at an Australian based ADI-Land Ordnance manufacturing facility.

Firstly, the quantitative and qualitative characterisation of this nitration unit must occur before its optimisation can begin. To characterise the nitration process, cutting-edge CFD technology, which when used judiciously, is known to have innocuous impact on human safety, the environment and economic factors. In this research work, steady-state and transient simulations were conducted using commercially available Fluent® CFD processor/post-processor V6.2.16 and GAMBIT V2.2.30 pre-processor. This software is based on the Finite Volume (FV) method

which uses the integral form of the conservation of equations as its starting point to ensure global conservation. A differential equation is integrated over the volume of each cell to obtain algebraic equations. Variable values are stored at the cell centres and interpolation using Taylor series expansion is used to express variable values at cell faces in terms of the cell centre values. Surface and volume integrals are estimated using appropriate quadrature formulae. As a consequence, all algebraic equations per cell are obtained in which a number of neighbouring cell centre values appear as unknowns. As FV method can accommodate any type of grid it is therefore suitable for handling complex geometry such as the nitration unit. In addition, the Multiple Reference Frame (MRF) approach was used to model and simulate the rotation of the impeller inside the nitration unit.

CFD will provide velocity flow fields that enable us to predict whether the nitration unit can be optimised. The validation of our CFD simulation results with the 7-equations Reynolds Stress Models (RSM) was achieved by comparing them to physical experimental results obtained through the use of PIV technology. In general, many researchers reported great success with laminar flow modelling [2] However, other researchers claimed that although CFD accurately predicted, both qualitatively and quantitatively, the axial-radial mean flow fields under- or over-predicted the tangential velocity component and turbulent quantities such as the turbulent kinetic energy, *k* and the turbulent energy dissipation rate, ε [3-4]. Hitherto, most of the research was conducted on bench scale equipment confined to studies involving solids suspension, liquid-liquid mixing or gas dispersion. Very few studies studied the drawdown of floating solids [5], even though such a process is important in food processing, polymerisation reactions and fermentation processes. This study aims to fill this research gap and to use the available information for the subsequent optimisation of our unit operation.

Chemicals consisting of 61% concentrated nitric acids (HNO_3), 29% concentrated sulphuric acid (H_2SO_4) and 10% H_2O were being used to nitrate the Alpha Cellulose Boards (ACB), 2% w/w to nitrocellulose. Nitrocellulose is a highly flammable energetic compound manufactured by nitration of ACB with HNO_3, in the presence of H_2SO_4, that is:

$$\mathbf{C_6H_{10}O_5 + xHNO_3 \Leftrightarrow C_6H_{10-x}O_{5-x}(ONO_2)_x + xH_2O}$$

This nitration process adds a large amount of O_2 to the chemical structure of the cellulose.

Most chemical reactor design is greatly dependent on mixing and contacting, which are very fundamental steps in any chemical reaction. Reactants must first be brought together for a chemical reaction to occur since without mixing and contacting no chemical reaction can take place. The primary design objective for chemical reactors from a mixing and contacting perspective is to obtain a kinetically controlled or equilibrium-controlled reactor and to eliminate all limitations due to transport. Similarly, to enhance the rate of nitration, it is essential that any mass transfer limitation be eliminated or minimised. For nitration to take place, mass transfer from the bulk liquid to the immediate region surrounding the ACB particles must occur. The fluid surrounding the particles will react with the ACB and be depleted. To ensure continuous high nitration rate is maintained, these depleted mixed acids must be replaced with fresh acid from the bulk fluid. Thus, one obvious way to maintain high nitration rate is to increase the relative velocity between the mixed acids and the ACB particles. This in turn can be achieved by

investigating methods to induce high turbulence and minimise zones of low turbulence. It is well known from physical experiment measurements and CFD simulations that the turbulence flow profile is far from homogeneous. Significant variations exist in the state of turbulence at different positions within the nitration tank, from the impeller region to the bulk liquid. These variations will affect the local mass transfer rate which eventually affects the global rate of nitration.

PROJECT GOALS

It is the intention of this study to model and simulate this nitration unit where nitration process is taking place with a view to quantifying its characteristics using parameters such as the power number, flow number, flow efficiency, blending time, percentage deviation from ideality and to provide qualitative information pertaining to the flow field for velocity, turbulence kinetic energy and its dissipation rates. Such information will then be used to optimise its performance.

In this paper, the authors present:

1. Simulation results obtained by modelling a scaled-down version of the nitration unit, validated using PIV;
2. Simulation results obtained using the same approach, on the actual nitration unit, for the purpose of characterising its performance
3. Simulation results that discovered the geometrical configuration which promises optimum performance

The validation of CFD results is important to instil confidence among the stakeholders and to prove that the models employed are robust and reliable enough to capture the hydrodynamics behaviour. Thus validation study was conducted prior to modelling and simulating the actual industrial size nitration unit. Most validated mixing tank were set on a baffled system [6-8] using liquid water as the medium. Very few studies have been conducted on unbaffled mixing tank. Besides fulfilling ADI's commercial need, the aim of this paper is to fill this research gap. To ensure the integrity of the models, validation by means of using a scaled-down version of the nitration unit and applying advanced physical experiments utilising PIV technology was conducted. Validation of CFD results using PIV for the purpose of thorough analysis using the existing industrial scale version was not possible owing to its opaque wall which blocks laser light transmission. Nonetheless, to overcome this shortcoming, a scaled-down version of this unit having dimensions 0.5 of the actual industrial size was built. The unit was made from Perspex which allows PIV to capture any insidious flow profile and to measure the mean velocity components inside the tank, as shown in Figure 1. The tank used was unbaffled, dished bottom, has a volume of 100L, is surrounded by transparent rectangular Perspex wall, and is filled with water, to minimise light refraction. Two impellers, attached to a single top-shaft were used. The top impeller was a standard pitch-blade turbine (PBT) while the bottom impeller consisted of two 90^{o} vertical blades and two 45^{o} blades. Two impellers are required in this case due to the multiple objectives, that is, floating particles drawdown and to keep particles fully suspended. The top impeller promotes ACB drawdown while the bottom impeller is to ensure the wetted ACB, having density heavier than its continuous medium, completely suspended. The

scaled-down unit was meshed, as shown in Figure 2, using mainly hexahedral cells to ensure faster convergence and to produce highly accurate results.

Figure 1: The scaled-down unit made from Perspex

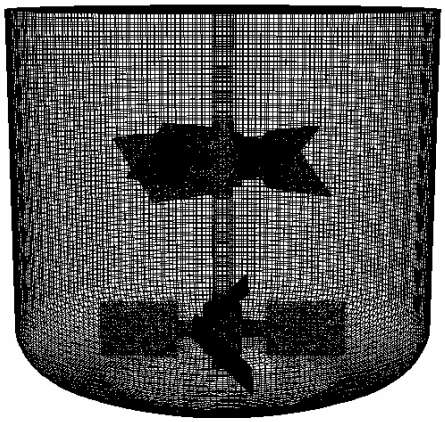

Figure 2: Meshed model of nitration unit

PIV EXPERIMENT SETUP

In this technology, multiple images of tracer materials (20micron Rhodamine B based fluorescent particles) distributed homogeneously (3mg/100L) in the water medium were captured. Since the tracer particles having density of 1050kgm^{-3} have almost similar physical properties to that of H_2O, they do not alter the flow field. Because of this, local fluid velocity can be calculated by measuring the fluid displacement from multiple particle images and dividing that displacement by the time interval between the exposures.

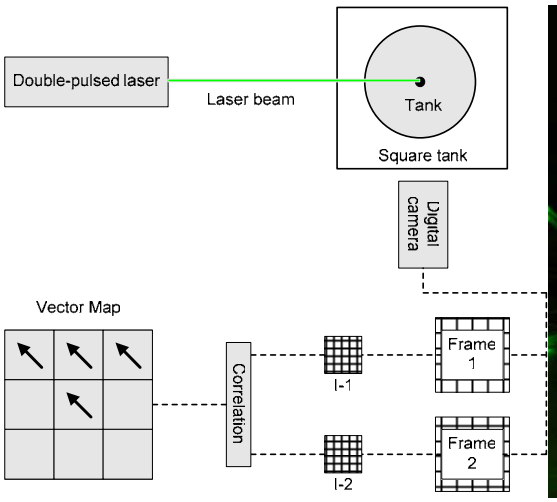

Figure 3: PIV setup

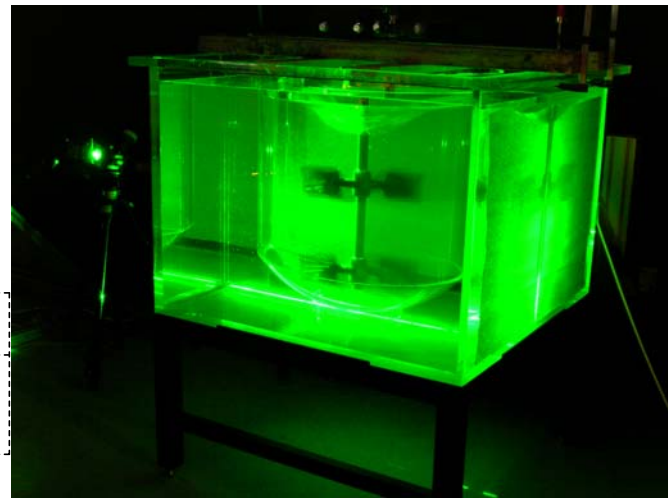

Figure 4: Scaled-down unit under laser illumination

Figure 3 shows the setup of the PIV experiment whereby a pair of pulsed lasers (532nm) emitted by laser generator (New Wave Research), separated by 3 milliseconds, were used to provide the pulsed light sheet illumination. When a pair of laser pulses was beamed to the target area, only the tracer particles became illuminated since other structures have been treated so as not to

reflect the laser beam. A digital camera (Nikon Sensicam, 12-bit cooled imaging charged-coupled device) located perpendicular to the plane of the light sheet was used to capture and transform the target area onto the camera array. This enables the camera to capture each light pulse in separate image frames. Once a sequence of 400 light pulses was recorded, the images were divided into small subsections called the interrogation areas (I). Each interrogation area (I-1 & I-2) was cross-correlated with each other, pixel by pixel. The correlation produced a signal peak, identifying a particle displacement, Δx. A velocity vector map over the whole target area was obtained by repeating the cross-correlation for each interrogation area over the 400 image frames captured by the camera. The velocity magnitude was obtained by averaging the velocity registered by each frame over the entire 400 frames. Figure 4 shows a laser illuminated scale-down unit with the impeller rotating at 33rpm, surrounded by a rectangular tank filled with water, which was needed to minimised laser refraction. CFD results and those from PIV experiment were compared by sampling the velocity at different position in the tank.

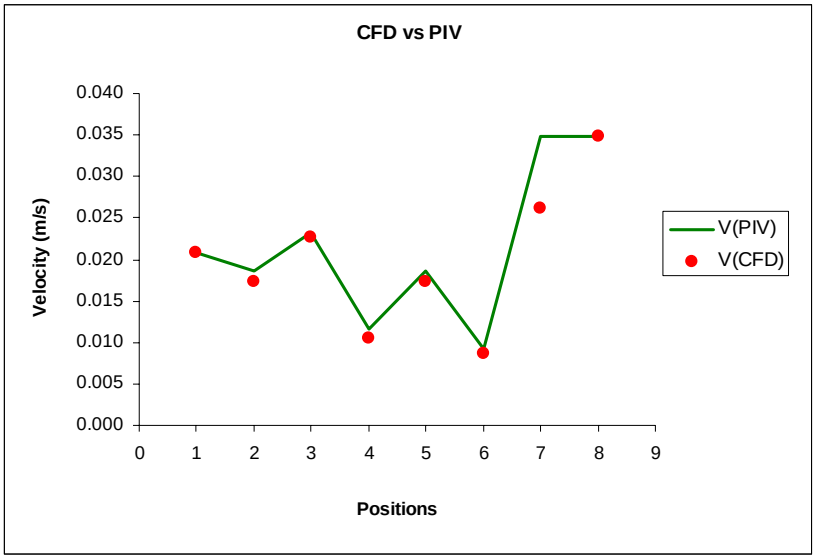

Figure 5: Velocity comparison between CFD and

Figure 5 shows that with exception of position 7, the CFD results were in close agreement with those obtained via PIV experiment. Position 7 shows that CFD underpredicted the PIV results by as much as 25%. The authors felt that this could be attributed to the free surface that affects the drawdown velocity. Details of this validation work can be found in [1].

THEORETICAL CONSIDERATION

Unlike the k-e model which assumes isotropic turbulence and therefore may not be well suited to flows in which the anisotropy of turbulence significantly affects the mean flow. Since the RSM accounts for the effects of streamline curvature, rotation, swirl, rapid changes in the rate of strain, in a more rigorous manner than the one-equation and two-equation models, therefore the RSM model has a greater potential to provide a more accurate prediction for complex flow. Thus, to model the existing unbaffled-nitration unit, the Reynolds stress models (RSM), even though it is the most computationally expensive model, is the most suitable model for this application and our aim for accuracy. The RSM transport equation [9] is given by:

$$\frac{\partial}{\partial t}(\rho\overline{u_i'u_j'}) + \frac{\partial}{\partial x_k}(\rho u_k\overline{u_i'u_j'}) = -\frac{\partial}{\partial x_k}\left[\rho\overline{u_i'u_j'u_k'} + \overline{p(\delta_{kj}u_i' + \delta_{ik}u_j')}\right]$$

$$+\frac{\partial}{\partial x_k}\left[\mu\frac{\partial}{\partial x_k}(\overline{u_i'u_j'})\right] - \rho(\overline{u_i'u'}_k\frac{\partial u_j}{\partial x_k} + \overline{u_j'u_k'}\frac{\partial u_i}{\partial x_k}) - \rho\beta(g_iu_j'\theta + g_ju_i'\theta)$$

$$+\overline{p(\frac{\partial u_i'}{\partial x_j} + \frac{\partial u_j'}{\partial x_i})} - 2\mu\overline{\frac{\partial u_i'}{\partial x_k}\frac{\partial u_j'}{\partial x_k}} - 2\rho\Omega_k(\overline{u_j'u_m'}\varepsilon_{ikm} + \overline{u_i'u_m'}\varepsilon_{jkm})$$

The first two terms on the left hand side are the local time derivative and convection term while the remaining 7 terms on the right hand side are the turbulent diffusion, molecular diffusion, stress production, buoyancy production, pressure strain, dissipation and production by system rotation. Of the various terms in these equations, the convection, molecular diffusion, stress production and production by system rotation do not need any modelling. However, turbulent diffusion, buoyancy production, pressure strain and the dissipation term need to be modelled to close the equations.

On the other hand, to model the improved nitration unit fitted with four narrow baffles, Realizable k-e model [9] was used to capture the hydrodynamics. The Realizable k-e transport equation is given by:

$$\frac{\partial}{\partial t}(\rho k) + \frac{\partial}{\partial x_i}(\rho k u_j) = -\frac{\partial}{\partial x_i}\left[(\mu + \frac{u_t}{\sigma_k})\frac{\partial k}{\partial x_j}\right] + G_k + G_b - \rho\varepsilon - Y_M + S_k$$

and

$$\frac{\partial}{\partial t}(\rho\varepsilon) + \frac{\partial}{\partial x_j}(\rho\varepsilon u_j) = -\frac{\partial}{\partial x_j}\left[(\mu + \frac{u_t}{\sigma_\varepsilon})\frac{\partial \varepsilon}{\partial x_j}\right] + \rho C_1 S_\varepsilon - \rho C_2\frac{\varepsilon^2}{k + \sqrt{v\varepsilon}} + C_{1\varepsilon}\frac{\varepsilon}{k}C_{3\varepsilon}G_b + S_\varepsilon$$

In the two equations above, G_k represents the turbulence kinetic energy generated due to the mean velocity gradients whereas G_b is the turbulence kinetic energy due to buoyancy. Y_M represents the contribution of the fluctuating dilation in compressible turbulence to the overall dissipation rate. C_2 and $C_{1\varepsilon}$ are constants; σ_k and σ_ε are the turbulent Prandtl numbers for k and ε respectively.

CHARACTERISATION OF NITRATION UNIT

After the successful validation of the scaled-down unit, the actual industrial size nitration unit was modelled and simulated using the same approach. The nitration unit has geometry identical to that used in the validation study. The only differences were: the actual unit has a volume 5 times larger, the tank wall was made of stainless steel and the fluid used was the process chemicals. Table 1 summarises the geometrical configuration and its operating parameters of the existing nitration unit.

Table 1: Actual nitration unit dimension and operating parameters

PARAMETER	VALUES	PARAMETER	VALUES
D/T	0.6	Density, ρ @ 32^{o}C	1713 kgm^{-3}
C/T	0.162	Viscosity @ 32^{o}C	0.010577 kgm^{-1}s^{-1}
W/D	0.135 (90^{o}) & 0.185 (45^{o})	Gravity	9.81ms^{-2}
T	1,000mm	Operating pressure	101325 Pa
S/D	0.7	Impeller speeds, N	73 rpm
V/D	0.5	Rotation direction	clockwise
Fluid	HNO_3-H_2SO_4-H_2O	Batch volume	676L

(D: impeller diameter, T: tank diameter, C: impeller bottom clearance, W: impeller blade width, S: impellers spacing, V: impeller top clearance)

RESULTS AND DISCUSSION

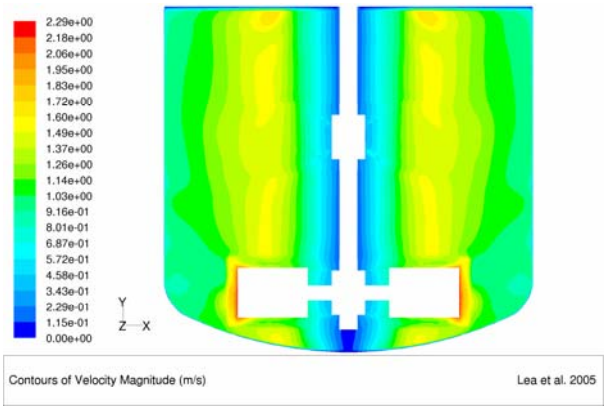

Figure 6: Contours of velocity magnitude

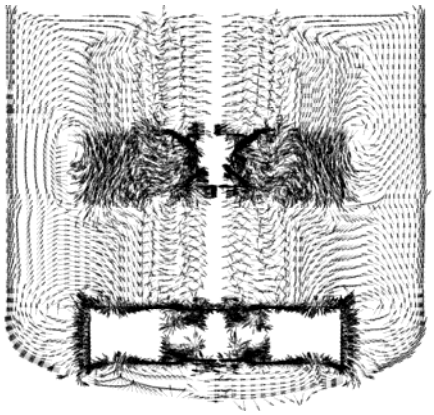

Figure 7: Flow field, axial plane

Figure 6 shows that the two impellers mounted on the same shaft directed the flow downwards towards the tank bottom. The profile shows the axial nature of the flow profile which reflects the kind of impellers used. Figure 7 shows that fluid was drawn down by the top impeller and discharged to the bottom impeller. At the bottom impeller, because of the 90^{O} vertical blades and the close proximity of this impeller to the tank bottom, the discharge was directed radially towards the tank wall. The fluid along the wall moves up where it is drawn down again. Ideally, only one large swirl loop should exist but due to the employment of two impellers in a tank with an aspect ratio, H/T≤1.2, two visible swirl loops, one next to the bottom blade and the other next to the top impeller existed. Current design utilised two impellers since there were multiple objectives, that is, floating solids drawdown and wetted solids suspension. Employing two

impellers means the flow complexity has been greatly increased especially when there was interaction between the flows generated by the two impellers. The extent of interaction depends on the impeller spacing. Since the impeller spacing ratio, S/D<1, higher shear zone is expected in the region between the two impeller. However, it is worthwhile to consider and investigate ways to reduce this to one impeller. The impeller top clearance, V/D=0.5 may not yield an optimum process result since the surface vortex is deep enough to cause air entrainment. Ideally, V/D≥0.5 for a system that employs standard baffle (T/12) and V/D≥1.0 for a system employing narrow baffles (T/50).

The axial mass flowrate discharged by both the top and bottom impellers were 60.93kgs^{-1} and 56.85kgs^{-1} respectively. Even though this calculation indicated that the bottom impeller flow discharged almost the same amount of fluid axially, it must be reminded that much of the fluid discharged from the top impeller went through the bottom impeller thus producing a higher impeller discharge value for the bottom impeller. To provide a clearer picture, cylindrical surfaces surrounding each impeller were integrated and the radial mass flowrate discharged by the top and bottom impellers were calculated to be 32.23kgs^{-1} and 83.39kgs^{-1} respectively. This shows that while the value for the top impeller looks satisfactory, the bottom impeller values indicates otherwise, the reason being, it is desirable to have an axial flow impeller at the bottom to sweep the tank bottom off the solid particles. However in this case, not only did the 90^{o} vertical blades reduce the axial flow component, they also contributed to the unnecessary excess fluid body rotation where in the absence of baffles, led to a marked reduction in turbulence kinetic energy. Even though the pitch blade turbine is a mixed flow impeller, at D/T > 0.55, the flow discharge becomes radial. Thus, one way to increase the axial flow discharge of both impellers is to reduce the D/T ratio. But a balance must be achieved between low D/T ratio and power consumption since impellers with a small D/T ratio often require higher rotational speed, thus higher power to achieve the process objective.

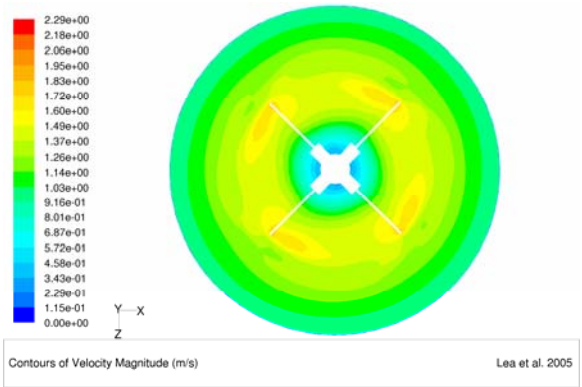

Figure 8: Contours of velocity magnitude

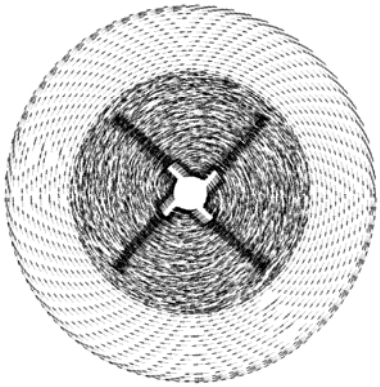

Figure 9: Flow field, radial plane

Figure 8 shows that the velocity magnitude initially increases with distance from the shaft and decreases as it moves, in a radial direction, further away from the blades towards the wall. Figure 9 shows that even though the process takes place at turbulence regime, the flow exhibited 'laminar' like characteristics due to the absence of wall baffles.

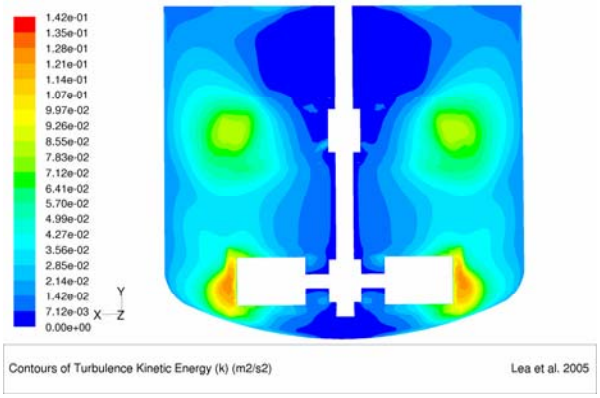

Figure 10: Contour, axial plane

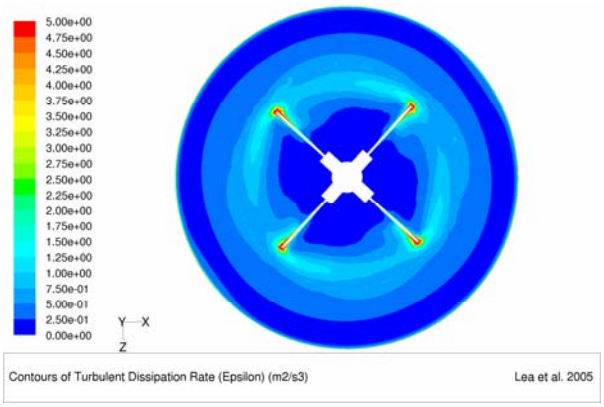

Figure 11: Contour, radial plane

Figure 10 shows that the turbulence kinetic energy, at 73 rpm, varies from one region of the tank to another. The figures also show that the turbulence kinetic energy around the wall is lowest that could be due to the lack of baffles, leading to high rotational flow, as confirmed by Figure 11, which shows the uninterrupted rotational flow of the fluid medium. Unbaffled tank which causes high rotational flow, minimises turbulence and inhibits top-to-bottom turnover rarely finds industrial application except in situation that demands high rate of heat transfer from the unit to the atmosphere. As such, this rotational flow coupled with the fact that the unit is unjacketed acted counter-productive to one of the process objectives of keeping a constant operating liquid bulk temperature. The region just above the top impeller represents a deep central vortex and the area just below the bottom impeller represents a zone of low velocity flow. This undesired zone could be attributed to the overly close bottom impeller clearance which then caused the flow to become radial even though two of the four blades were supposed to produce axial flow pattern. In addition, the impeller design that incorporates a bridge linking the blades to the hub may partly be the reason for the existence of this zone.

Figure 11 shows that most of the energy was dissipated around the impeller tips and that very little energy has been imparted to the fluid starting from the shaft to midway of the impeller.

OPTIMISATION STRATEGY

Now that the nitration unit has been characterised, different geometrical configurations will be simulated using the same CFD package with a view to optimising the performance of this nitration unit. Keeping other parameters constant, simulations involving different geometrical configurations focussing on the impellers and baffles were carried out. For impellers, the impact of using different types of impeller designs, various levels of D/T, W/D, C/T, S/D and V/D ratios, were studied. In addition, different number of baffles will be simulated. While one-factor at a time experiment is suitable for a characterisation study, it is insufficient for an optimisation study due to the existence of multivariable interactions between different parameters. Ideally, to capture the process fully, a full factorial experiment should be carried out but because full factorial experiment is too extensive, it is economically prohibitive, thus a fractional factorial design of experiment was used. The quantitative performance objectives are: power number (smaller is better), flow number (bigger is better) flow efficiency (bigger is better), flowrate

(bigger is better), blending time (smaller is better), deviation from ideality (smaller is better) and global turbulence (bigger is better).

As for the qualitative performance objectives, the flow field generated will be used to remove or minimise dead zones, to induce turbulence in areas of laminar-like zone and to direct the flow to areas which require high fluid flow such as the tank bottom. To achieve this, narrow baffles (T/50) will be simulated with a view to breaking the "laminar" rotational flow and to convert radial flow to axial flow. Installing narrow baffles will also reduce the formation of vortex, thus permitting operation at a higher impeller speed. To remove the dead zone and create a more homogenous mixture, different impeller designs will be simulated. Removing the dead zones will result in a more homogenous overall mixture which will eventually lead to a more uniform nitration rate throughout the entire nitration unit and resulting in a higher global nitration rate.

Table 2: Trial conditions

TRIAL #	**1**	**2**	**3**	**4**	**5**	**6**	**7**	**8**
No. of baffles	2	2	2	2	4	4	4	4
Impeller diameter	0.55T	0.55T	0.6T	0.6T	0.55T	0.55T	0.6T	0.6T
No. of impellers	1	2	1	2	1	2	1	2
Blade width	0.3D	0.35D	0.35D	0.3D	0.35D	0.3D	0.3D	0.35D

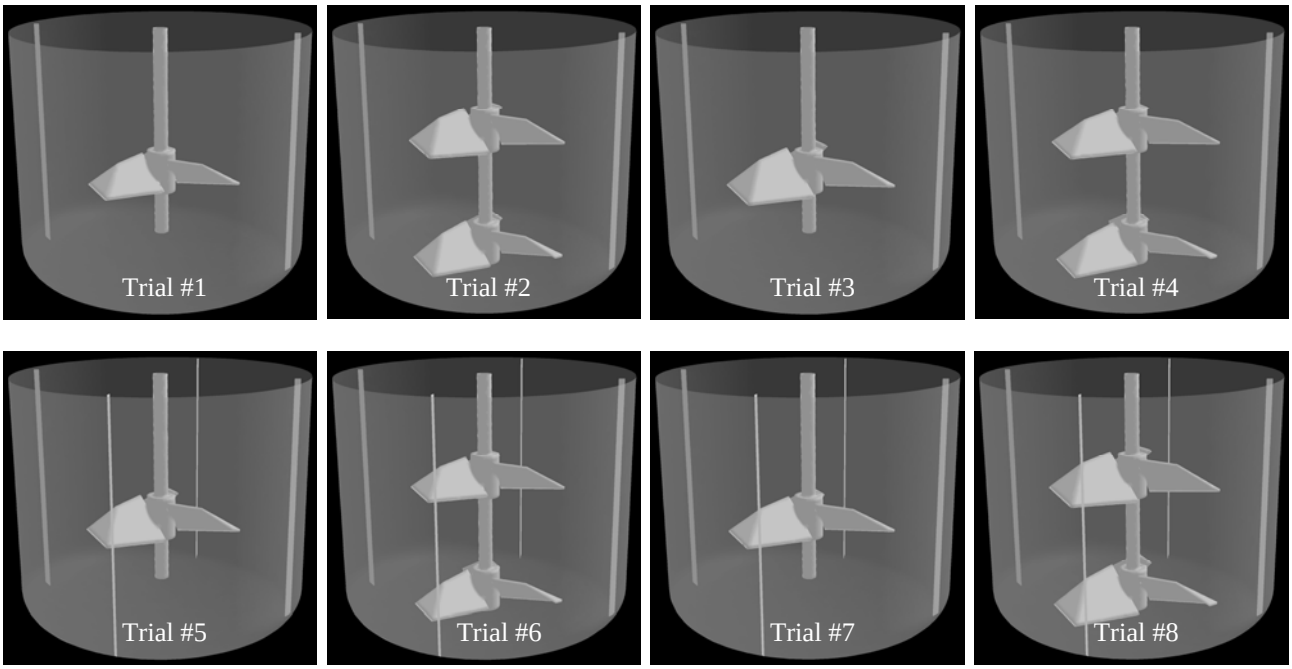

Figure 12: Different geometrical configurations

Table 2 summarises the trial conditions simulated while Figure 12 shows the diagrammatic representation of the trial conditions. Performance indicators for each conditions were compared and it was discovered that trial condition #6 yielded the best results.

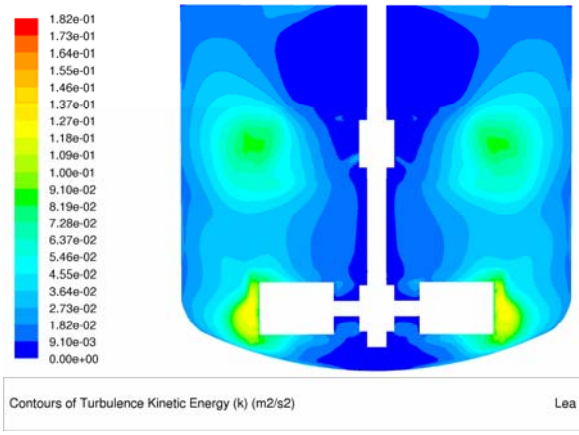

Figure 13: Existing system

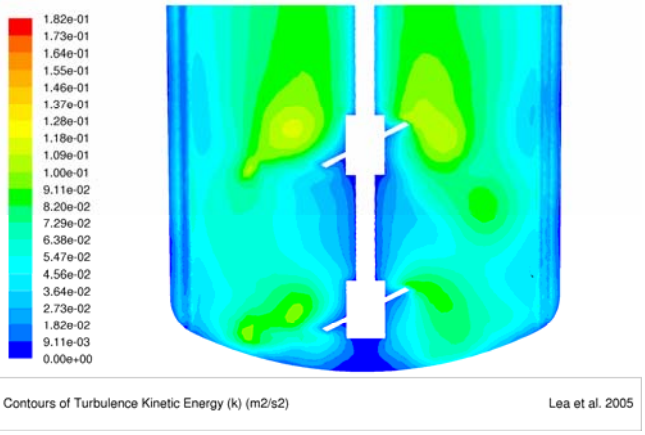

Figure 14: Proposed system

Existing system depicted by Figures 13 show that the lowest turbulence areas are confined to those above the impellers, around the shaft and at the tank bottom. With the proposed system, as shown in Figure 14 (trial condition #6) the areas of low turbulence above shown in the existing system vanished and the low turbulence region at the tank bottom was significantly minimised. Moreover, turbulence around wall region is higher relative to the existing system.

Table 3. Improvement expected with the proposed unit

PARAMETER	EXISTING	PROPOSED	IMPROVEMENT
Power number, N_P	0.6089	0.8243	35.38%
Flow number, N_Q	0.2615	0.603	130.59%
Flow efficiency, η	0.4295	0.7316	70.34%
Flow rate, kgs^{-1}	117.8	209.1	77.50%
Blending time, t_B, s	26.82	15.68	41.54%
Deviation from ideality, ξ	14.13%	4.53%	67.92%
Global turbulence, m^2s^{-2}	37,014	51,535	39.23%

Table 3 above shows the power number (Power/[$\rho \times N^3 \times D^5$]) increases by 35.38% which is due to the installation of four narrow baffles. Even though it is desirable to minimise power consumption, in some cases, more power is required to achieve process objective. In this case, a higher power consumed means more power is delivered into the process fluid. The flow number (Flowrate/[$\rho \times N \times D^3$]) has been increased to 130.59% at the same rotational speed and using a slightly smaller diameter impeller. The huge increase is attributed to the new impeller design and the installation of four narrow baffles which promote axial flow. Flow efficiency ([N_Q/N_P] $\times$100%) which increases by 70.34%, shows that the proposed system is much more power efficient than the existing system. High flowrate will help to promote the drawdown of floating ACB. Blending time was shortened by 41.54% which can be translated into a higher plant throughput. Deviation from ideality was reduced by 67.92% which mean the room for improving the blending time is now much smaller. Finally, the global turbulence for the proposed system exceeded that of the existing system by 39.23%, thus the mass transfer rate should increase significantly.

CONCLUSION

This paper has presented the application of cutting-edge CFD technology to characterise our nitration unit and to reveal important information which was otherwise latent without the application of CFD. To increase our confidence in the simulation results, the CFD results were validated against empirical results obtained from a scaled-down version of the actual nitration unit using PIV technology. Subsequent to the successful validation of the models and simulations, the performance of the actual nitration unit was characterised using the same approach. Both the quantitative and qualitative characterisation parameters were presented. With such intimate information, trial conditions each having a different geometrical configuration from the rest was simulated. Results show that the nitration unit fitted with two newly developed axial flow impellers and four narrow baffles distinctly outperformed the other geometrical configurations. This geometrical configuration was selected as the new nitration unit with its performance far exceeding the existing nitration unit.

REFERENCES

1. Lea J., Gehrig A., Flavel P. and Adesina A.A. [2005], The computational fluid dynamics modelling and simulation of nitration unit employed for the manufacture of military propellant, ICCHMT May 17-20 2005, Paris, France
2. Lamberto D.J., Alvarez M.M. and Muzzio F.J. [1999], Experimental and computational investigation of the laminar flow structure in a stirred tank, Vol 54, 919-942, Chemical Engineering Science
3. Sheng J., Meng H. and Fox R.O. [1998], Validation of CFD simulations of a stirred tank using particle image velocimetry data, Vol 76, 611-625, The Canadian Journal of Chemical Engineering
4. Montante G., Lee K.C., Brucato A. and Yianneskis M. [2001], Numerical simulations of the dependency of flow pattern on impeller clearance in stirred tank, Vol 56, 3751-3770, Chemical Engineering Science
5. Ozcan-Taskin G. & Wei H. [2003], The effect of impeller-to-tank diameter ratio on draw down of solids, Vol 58, 2011-2022, Chemical Engineering Science
6. Xuereb C. and Bertrand J. [1996], 3-D hydrodynamics in a tank stirred by a double-propeller system and filled with a liquid having evolving rheological properties, Vol 51, 1725-1734, Chemical Engineering Science
7. Harvey III A.D., Wood S.P. and Leng D.E. [1997], Experimental and computational study of multiple impeller flows, Vol 52, 1479-1491, Chemical Engineering Science
8. Revstedt J., Fuchs L., Kovacs T. and Tragardh C. [1998], Large eddy simulations of the turbulent flow in a stirred reactor, Vol 53, No 24, 4041-4053, Chemical Engineering Science
9. Ranade V.V. [2002] Computational flow modelling for chemical reactor engineering, Academic Press, Process Systems Engineering, Vol 5

ACKNOWLEDGEMENT

Special thanks go to Mr Patrick O'Flaherty and Ms June Dous (ADI-Human Resources)

Contributions from the following individuals are duly noted:
Mr Howard Brettig and Mr Robert Hamson (ADI-New Capabilities)
Mr Hung Chau and Ms Katia Nassev (UNSW-IA Laboratory)